Polymorphism Control And Dissolution Enhancement Of Ritonavir Via Amorphous Solid Dispersion-Based Tablet Formulation

Sachin Bhagwat Aglawe[1], Sakshi Ganesh Lokhande[1*], Vijay Bhausaheb Jadhav[1], Nitin Pannalal Jain[1], Usha Nitin Jain[1], Karveer Babanrao Aghade[1]

[1]Rashtrasant Janardhan Swami College of Pharmacy, Kokamthan, Tal-Kopargaon, Dist- Ahliyanagar, Maharashtra, India

*Corresponding Author: Sakshi Ganesh Lokhande, Rashtrasant Janardhan Swami College of Pharmacy, Kokamthan, Tal-Kopargaon, Dist- Ahliyanagar, Maharashtra, India, Email- lokhandesakshi1225@gmail.com

ABSTRACT

Ritonavir, a BCS Class IV HIV protease inhibitor, presents significant formulation challenges due to poor aqueous solubility, low oral bioavailability, and pronounced polymorphic behaviour. The conversion from metastable Form I to the thermodynamically stable but poorly soluble Form II has historically compromised bioavailability. This study aimed to enhance the solubility and dissolution of ritonavir through amorphous solid dispersions (ASDs) prepared by the solvent evaporation technique using hydroxypropyl methylcellulose K100 (HPMC K100) and polyvinylpyrrolidone K30 (PVP K30) as hydrophilic polymeric carriers.

Nine ASD formulations (F1–F9) were prepared at varying drug-to-polymer ratios and compressed into tablets using suitable excipients. Precompression parameters including bulk density, tapped density, Carr's index, Hausner ratio, and angle of repose were evaluated. Solid-state characterization was performed using FTIR spectroscopy and differential scanning calorimetry (DSC).

FTIR analysis confirmed physicochemical compatibility between ritonavir and the selected polymers, with slight peak shifting suggesting intermolecular hydrogen bonding interactions. DSC thermograms of pure ritonavir showed a sharp endothermic melting peak at 124.80°C, confirming its crystalline nature. This peak was absent in all ASD formulations, confirming successful amorphous conversion. Drug content analysis demonstrated satisfactory uniformity with 98.77% purity.

In vitro dissolution studies revealed significantly enhanced drug release from all ASD formulations compared to pure crystalline ritonavir. Formulation F6 exhibited the highest cumulative drug release of approximately 104% at 30 minutes. The enhanced dissolution was attributed to amorphous conversion, improved wettability, increased surface area, and effective polymer-drug interactions. The study conclusively demonstrates that solvent evaporation-based ASD technology is an effective an0d promising strategy for improving the dissolution and oral delivery of ritonavir.

Keywords: Ritonavir, Polymorphism, Amorphous Solid Dispersion, HPMC K100, PVP K30

Introduction

Background and Significance

The pharmaceutical industry continues to face a persistent challenge: poor aqueous solubility of newly discovered drug candidates. Approximately 40–70% of new chemical entities identified through combinatorial screening are poorly water-soluble, limiting their translation into viable drug products. Oral bioavailability is critically dependent upon adequate drug dissolution in the gastrointestinal tract, and when solubility is limiting, even well-absorbed molecules fail to achieve therapeutic plasma concentrations[1]. Ritonavir stands as a landmark case study in pharmaceutical development. Approved by the US FDA in 1996 as the first HIV protease inhibitor, its commercial success was disrupted in 1998 when a thermodynamically more stable polymorph (Form II) spontaneously crystallized within the formulation, dramatically reducing bioavailability and forcing temporary market withdrawal. This event underscored the necessity of rigorous polymorphic characterization during pharmaceutical development[2].

Ritonavir: Physicochemical Properties and Challenges

Ritonavir ($C_{37}H_{48}N_6O_5S_2$; MW: 720.94 g/mol) is a peptidomimetic HIV-1 and HIV-2 protease inhibitor classified as a BCS Class IV compound, exhibiting poor aqueous solubility (approximately 1.3 µg/mL at 25°C) and poor intestinal permeability. Form II, discovered in 1998, is approximately 50% less soluble than the original Form I, directly reducing oral bioavailability and necessitating reformulation into a self-micro emulsifying drug delivery system (SMEDDS). Additionally, extensive first-pass metabolism by CYP3A4 and high lipophilicity (log P ≈ 5.98) further compromise bioavailability, making ritonavir an ideal candidate for advanced solubility enhancement strategies[3].

Polymorphism in Pharmaceutical Science

Polymorphism refers to the ability of a solid material to exist in more than one crystalline form. Different polymorphs share identical chemical composition but differ in crystal lattice arrangement, resulting in distinct properties including melting point, solubility, and dissolution rate — differences that directly impact bioavailability and therapeutic efficacy. Metastable polymorphs tend to be more soluble but may convert to stable, less soluble forms under the influence of temperature, humidity, mechanical stress, or drug-excipient interactions.

ICH Q6A mandates thorough polymorphic characterization using analytical tools such as DSC, XRPD, and IR spectroscopy[4].

Amorphous Solid Dispersions: Concept and Advantages

Amorphous solid dispersions (ASDs) represent one of the most clinically validated strategies for enhancing solubility of poorly water-soluble drugs. By disrupting the crystalline order of the drug and converting it to a higher-energy amorphous state, ASDs significantly improve apparent solubility and dissolution kinetics. The polymer matrix molecularly disperses the drug, eliminates the lattice energy barrier to dissolution, and prevents recrystallization. A key phenomenon in ASD dissolution is the "spring and parachute" effect, wherein rapid amorphous drug dissolution generates supersaturation, while the polymer suppresses crystallization to maintain supersaturation long enough for absorption to occur. Physical stability of ASDs is governed by the composite glass transition temperature (Tg), with systems exhibiting Tg values exceeding storage temperature by at least 50°C demonstrating superior stability[5].

Role of Polymeric Carriers in ASD

The selection of polymeric carrier is critical in ASD development, governing physical stability, dissolution performance, and processability. HPMC K100, a semi-synthetic cellulose derivative with a Tg of approximately 170–180°C, acts as a crystallization inhibitor through adsorption onto nucleating drug crystals and forms hydrogen bonds with ritonavir, promoting molecular-level drug-polymer miscibility. PVP K30, a synthetic hydrophilic polymer (MW ~40,000 Da, Tg ~175°C), enhances solubility through complexation, inhibition of nucleation, and rapid matrix dissolution. The combination of HPMC K100 and PVP K30 exploits complementary stabilization mechanisms, offering synergistic dissolution enhancement superior to either polymer alone[6].

Solvent Evaporation Method and Tablet Formulation

The solvent evaporation method achieves intimate molecular-level drug-polymer mixing in a common volatile solvent, which is then removed under controlled conditions to yield an amorphous dispersion. This method avoids high-temperature processing, making it suitable for thermolabile drugs. Methanol was employed as the solvent in the present study due to ritonavir's adequate solubility and methanol's low boiling point (64.7°C), enabling efficient evaporation at 40–45°C. The resulting ASD powder was subsequently compressed into tablets using mannitol as diluent, croscarmellose sodium as disintegrant, talc as glidant, and magnesium stearate as lubricant — excipients selected to preserve amorphous stability and support rapid dissolution[7].

Materials And Methods

Materials

Ritonavir active pharmaceutical ingredient (API) was procured from a certified pharmaceutical supplier and used as received. Hydroxypropyl methylcellulose K100 (HPMC K100; Methocel K100M, Dow Chemical Company) and Polyvinylpyrrolidone K30 (PVP K30; Kollidon 30, BASF SE) were obtained from their respective manufacturers as pharmaceutical-grade excipients. Methanol (analytical reagent grade, ≥99.8% purity) was sourced from Merck India Limited. Mannitol (Pearlitol SD200, Roquette Frères, France), croscarmellose sodium (CCS; Ac-Di-Sol, FMC BioPolymer), talc (pharmaceutical grade), and magnesium stearate (pharmaceutical grade) were obtained from commercial suppliers. All solvents and chemicals used were of analytical reagent grade or better. Purified water (USP grade, resistivity >18 MΩ·cm) was prepared in-house using a Milli-Q water purification system.

Preformulation Studies

Prior to formulation development, standard preformulation studies were conducted to characterize the physical properties of ritonavir API and to provide a basis for rational formulation design[8].

Organoleptic Properties

The organoleptic properties of ritonavir API, including appearance (color, form), odor, and texture, were evaluated visually and manually[9].

Solubility Studies

The solubility of ritonavir was assessed qualitatively in various solvents including water, methanol, ethanol, acetone, dichloromethane, and phosphate buffer (pH 6.8) by adding excess drug to each solvent and observing dissolution after 24 hours of constant stirring at 25°C[10].

Melting Point Determination

The melting point of ritonavir was determined using a digital melting point apparatus (Veego Model VMP-D) by observing the temperature range of complete melting of the crystalline API.

Establishment of Calibration Curve

Stock solution preparation: A primary stock solution of ritonavir (1000 µg/mL) was prepared by dissolving 100 mg of accurately weighed ritonavir API in 100 mL of methanol in a volumetric flask. A secondary stock solution (100 µg/mL) was prepared by appropriate dilution of the primary stock with phosphate buffer pH 6.8 containing 0.5% w/v sodium lauryl sulfate (SLS) as the dissolution medium[11].

Working solutions in the concentration range of 10–50 µg/mL were prepared by serial dilution of the secondary stock solution with the dissolution medium. The absorbance of each solution was measured at the wavelength of maximum absorption (λmax = 231 nm) using a UV-Visible spectrophotometer (Shimadzu UV-1800 or equivalent) against the dissolution medium as blank. Each concentration was measured in triplicate[12].
The calibration curve was constructed by plotting absorbance (Y-axis) against concentration in µg/mL (X-axis), and the linear regression equation was determined. The linearity was assessed by the coefficient of determination (R^2)[12,13,14].

Preparation of Amorphous Solid Dispersions
Amorphous solid dispersions of ritonavir with HPMC K100 and PVP K30 were prepared using the solvent evaporation method, employing methanol as the common organic solvent. The procedure was standardized as follows:
Accurately weighed quantities of ritonavir (100 mg) and the respective polymer(s) as per the formulation batch composition (Table 1) were taken[15]. The drug and polymer(s) were dissolved together in approximately 20 mL of methanol in a glass beaker. The mixture was stirred using a magnetic stirrer at 500 rpm for 20–30 minutes at ambient temperature to ensure complete dissolution and homogeneous mixing. The resulting clear solution was transferred to a clean, pre-weighed petri dish (approximately 10 cm diameter) and spread uniformly to form a thin film[16]. The petri dish was placed in a hot air oven maintained at 40–45°C for controlled solvent evaporation. Drying was continued until a constant weight was achieved, indicating complete solvent removal (approximately 24–48 hours, depending on the batch). The resultant solid film was carefully scraped from the petri dish surface using a stainless-steel spatula and transferred to a mortar. The solid mass was gently ground using a pestle and passed through a #60 mesh sieve (250 µm aperture) to obtain a uniform powder with consistent particle size distribution. The sieved ASD powder was stored in a sealed glass container with silica gel desiccant at ambient temperature (25 ± 2°C, <45% RH) until further use[17,18,19].

Characterization Studies
Differential Scanning Calorimetry (DSC)
DSC analysis was performed using the Shimadzu DSC-60 differential scanning calorimeter under the following experimental conditions. Sample weight: 5.000 mg (accurately weighed). Temperature program: heating from 30°C to 400°C at a heating rate of 10°C/min. Atmosphere: dry nitrogen gas purge at 50 mL/min flow rate. Reference: empty sealed aluminium pan of identical type. All samples were hermetically sealed in aluminium DSC pans using a crimping press prior to analysis[28,29]. DSC analyses were performed on three samples: (1) pure crystalline ritonavir (Ritonavir Plane), (2) a physical mixture of ritonavir with excipients in the formulation ratio (Ritonavir with Excipient Mix), and (3) the prepared ASD (F1 representative). The thermograms were analysed for the presence or absence of endothermic melting peaks, peak temperatures, onset temperatures, and enthalpy values to confirm amorphous conversion and assess drug-excipient compatibility[30].

X FTIR Spectroscopic Analysis
FTIR spectroscopy was employed to confirm the chemical identity of ritonavir API and to evaluate physicochemical compatibility between ritonavir and the polymeric carriers HPMC K100 and PVP K30 in the prepared ASD formulations. Spectra were recorded for pure ritonavir, pure polymers, a physical mixture, and representative ASD formulations in the range of 4000–400 cm^{-1} using the KBr pellet technique.

Pure Ritonavir
The spectrum of pure crystalline ritonavir showed sharp, well-resolved characteristic peaks: a broad N–H/O–H stretch at ~3355 cm^{-1}, a strong carbamate C=O stretch at ~1702 cm^{-1} (most diagnostic peak), C=N/aromatic C=C stretch at ~1619 cm^{-1}, and C–O–C asymmetric stretch at ~1235 cm^{-1}. The sharpness of all peaks confirmed the highly crystalline nature of the API, consistent with DSC findings.

Physical Mixture
The physical mixture spectrum showed a simple superimposition of individual component peaks without significant shifts, indicating the absence of meaningful molecular-level interactions upon simple blending. This spectrum served as the critical reference baseline for comparison with ASD formulations.

ASD Formulations
All ASD formulations showed a consistent and pronounced downward shift of the ritonavir carbamate C=O band from ~1702 cm^{-1} to approximately 1607–1665 cm^{-1}, representing a bathochromic shift of 37–95 cm^{-1}. This shift is direct spectroscopic evidence of hydrogen bond formation between ritonavir's carbamate carbonyl and the O–H/N–H groups of HPMC K100 and PVP K30. Concurrent broadening of the N–H/O–H stretching region further confirmed drug-polymer hydrogen bonding. General peak broadening and loss of sharpness across all ASD spectra indicated disruption of the crystalline lattice, consistent with amorphous conversion. Importantly, no new peaks attributable to chemical degradation or reactive incompatibility were observed in any formulation.

Conclusion from FTIR
FTIR analysis confirmed complete physicochemical compatibility between ritonavir and the HPMC K100/PVP K30 polymer system. The observed peak shifts confirmed that the solvent evaporation process induced molecular-level hydrogen bonding interactions between drug and polymers, which thermodynamically stabilize the

amorphous state and inhibit recrystallization. These findings are in direct agreement with DSC results confirming successful amorphous conversion of ritonavir in all ASD formulations.

Drug Content Assay

Drug content of the tablet formulations was determined by UV spectrophotometry. Twenty tablets from each batch were weighed and the average weight determined. An amount of tablet powder equivalent to 50 mg ritonavir was accurately weighed and transferred to a 100 mL volumetric flask. About 60 mL of methanol was added and the mixture was sonicated for 15 minutes to ensure complete drug extraction, followed by volume makeup with methanol. The solution was filtered through Whatman No[37]. 1 filter paper and the filtrate was appropriately diluted with the dissolution medium to obtain a concentration within the calibration range. Absorbance was measured at λ max 231 nm against a reagent blank. Drug content was calculated using the calibration curve[31].

Percentage purity was calculated using the following formula: % Purity = (Found Concentration / Theoretical Concentration) × 100. The assay factor (F) derived from the calibration curve: C = A × F, where C = concentration (µg/mL), A = absorbance, F = 18.20. For a measured absorbance of 1.954, the found concentration = 1.954 × 18.20 = 35.56 µg/mL, yielding a purity of 98.77%.

In Vitro Dissolution Study

In vitro dissolution studies of pure ritonavir and all prepared ASD tablet formulations (F1–F9) were carried out using a USP Type II (Paddle) dissolution apparatus (Electrolab TDT-08L). The dissolution studies were performed in 900 mL phosphate buffer pH 6.8 containing 0.5% w/v sodium lauryl sulphate (SLS) maintained at 37 ± 0.5°C with a paddle rotation speed of 50 rpm[35,36]. At predetermined time intervals of 5, 10, 15, 20, 30, 45, 60, 90, and 120 minutes, 5 mL samples were withdrawn from the dissolution medium and immediately replaced with an equal volume of fresh dissolution medium maintained at the same temperature to preserve sink conditions. The withdrawn samples were filtered through a 0.45 µm membrane filter and analysed spectrophotometrically at 231 nm using a UV-visible spectrophotometer[32]. The cumulative percentage drug release (%CDR) was calculated using the previously prepared calibration curve of ritonavir. Dissolution profiles of pure ritonavir and all ASD tablet formulations (F1–F9) were compared to evaluate the effect of different polymer ratios and polymer combinations on the dissolution enhancement of ritonavir[33,34].

Table 1: Batch Composition of Ritonavir ASD Formulations (F1–F3)

Batch	Drug: HPMC:PVP Ratio	Ritonavir (mg)	HPMC K100 (mg)	PVP K30 (mg)
F1	1:1:1	100	100	100
F2	1:2:1	100	200	100
F3	1:1:2	100	100	200

Tablet Formulation

The ASD powders (equivalent to 100 mg ritonavir) were blended with the tablet excipients and compressed into tablets using a rotary tablet press. The formulation composition for each batch is provided in Table 2.

Table 2: Tablet Formulation Composition per Tablet

Ingredients	F1	F2	F3	F4	F5	F6	F7	F8	F9
Ratio Group	**1:1:1**	**1:1:1**	**1:1:1**	**1:2:1**	**1:2:1**	**1:2:1**	**1:1:2**	**1:1:2**	**1:1:2**
ASD Powder (mg)	**300**	**300**	**300**	**400**	**400**	**400**	**400**	**400**	**400**
Mannitol (mg)	**180**	**170**	**160**	**80**	**70**	**60**	**80**	**70**	**70**
CCS (mg)	**10**	**20**	**30**	**10**	**20**	**30**	**10**	**20**	**20**
Talc (mg)	**5**	**5**	**5**	**5**	**5**	**5**	**5**	**5**	**5**
Magnesium Stearate (mg)	**5**	**5**	**5**	**5**	**5**	**5**	**5**	**5**	**5**
Total Tablet Weight (mg)	**500**	**500**	**500**	**500**	**500**	**500**	**500**	**500**	**500**

Results And Discussion

Calibration Curve and Method Validation

The UV absorption spectrum of ritonavir in phosphate buffer pH 6.8 containing 0.5% SLS showed a characteristic λmax at 231 nm, corresponding to π→π* electronic transitions in the aromatic chromophore. Calibration solutions over 10–50 µg/mL demonstrated excellent linearity following Beer-Lambert's Law, with regression equation $A = 0.0550 \times C - 0.0017$ and $R^2 = 0.9998$. The method demonstrated acceptable accuracy, precision, and specificity for ritonavir quantification. Using the derived assay factor (F = 18.20), a measured absorbance of 1.954 corresponded to a drug concentration of 35.56 µg/mL, confirming a purity of 98.77%.

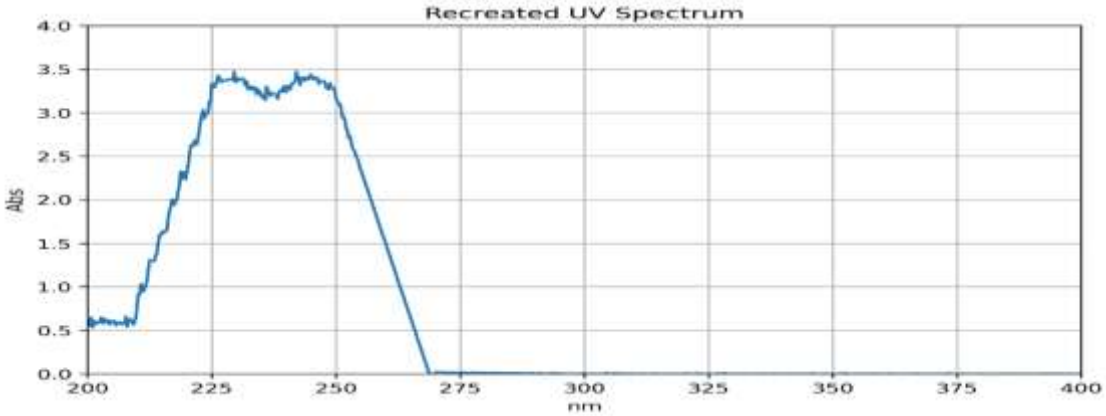

Figure 1 - UV absorption spectrum showing strong absorbance in the 220–255 nm region with rapid baseline decline beyond 270 nm

Preformulation Evaluation of Ritonavir

Preformulation evaluation results for all nine ASD powder batches are summarized in Table 3. The 1:2:1 ratio group (F4–F6) consistently exhibited the best powder flow characteristics, with F5 achieving an 'Excellent' flow rating based on Carr's index of 12.5%, Hausner ratio of 1.14, and angle of repose of 25.8°, attributed to higher HPMC K100 content imparting regular particle morphology and improved surface properties. The 1:1:1 group (F1–F3) demonstrated 'Good' flow, while the 1:1:2 group (F7–F9) showed 'Fair' flow, likely due to particle agglomeration resulting from the hygroscopic nature of higher PVP K30 content.

Table 3: Preformulation Evaluation Results for Ritonavir F1–F9

Parameter	**F1**	**F2**	**F3**	**F4**	**F5**	**F6**	**F7**	**F8**	**F9**
Bulk Density (g/mL)	0.46±0.02	0.47±0.05	0.45±0.02	0.48±6.02	0.49±0.02	0.48±0.02	0.44±0.02	0.45±0.02	0.46±0.02
Tapped Density (g/mL)	0.054±0.02	0.55±0.02	0.53±0.02	0.55±0.02	0.56±0.02	0.55±0.02	0.53±0.02	0.54±0.02	0.55±0.02
Carr's Index (%)	14.8±0.8	14.5±0.7	15.1±0.9	12.7±0.6	12.5±0.5	12.9±0.6	17.0±1.0	16.6±0.9	16.3±0.8
Hausner Ratio	1.17±0.02	1.17±0.01	1.18±0.02	1.14±0.01	1.14±0.01	1.15±0.01	1.20±0.02	1.19±0.02	1.19±0.02
Angle of Repose (°)	28.5±1.5	27.8±1.1	29.2±1.3	26.5±1.0	25.8±0.9	26.2±1.0	31.5±1.4	30.8±1.3	30.2±1.2
Flow Property	Good	Good	Good	Good	Excellent	Good	Fair	Fair	Fair

FTIR Spectroscopic Analysis

FTIR spectroscopy was employed to: (a) confirm the identity of pure ritonavir API through its characteristic absorption bands, and (b) assess potential chemical interactions between ritonavir and the HPMC K100/PVP K30 polymers in the ASD formulations. Four FTIR spectra were recorded and are presented below with detailed interpretation.

FTIR Spectrum of Pure Ritonavir (RTV.0)

The FTIR spectrum of pure crystalline ritonavir is presented in Figure 1. Key characteristic absorption bands are identified at the following wavenumbers:

• 3355.94 cm^{-1}: Broad O–H/N–H stretching vibration, characteristic of the carbamate NH and hydroxyl groups present in the ritonavir molecule.

• 1702.98 cm^{-1}: Strong C=O stretching of the carbamate functional group (urethane linkage). This is a highly diagnostic peak for ritonavir.

• 1619.56 cm^{-1}: C=N stretching or aromatic C=C stretching associated with the thiazole rings of ritonavir.

• 1377.75 cm^{-1}: C–H bending (methyl groups) and C–N stretching.

• 1235.65 cm^{-1}: C–O–C asymmetric stretching of the carbamate group.

• 1052.82 cm^{-1}: C–O stretching and C–N stretching vibrations.

• 948.26, 756.47, 598.67, 565.03 cm^{-1}: Various C–H out-of-plane bending and fingerprint region peaks characteristic of the aromatic rings and thiazole moieties.

The sharp, well-defined peaks in the spectrum confirm the crystalline nature of the pure API. The transmittance range of approximately 80–99% indicates high spectral quality.

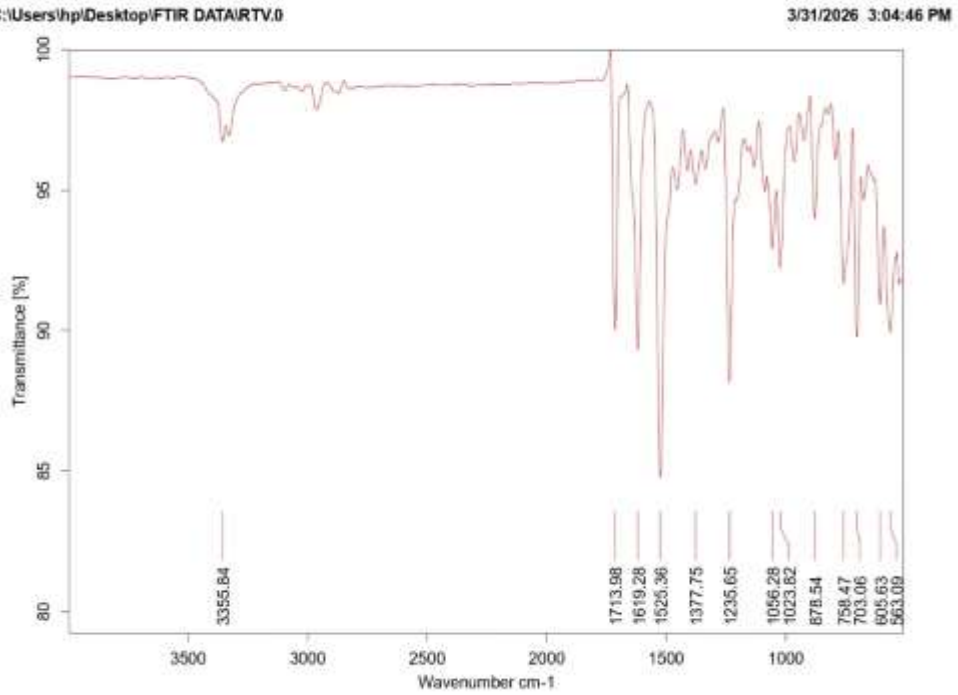

Figure 2: FTIR Spectrum of Pure Ritonavir API (RTV.0) – Recorded 31/03/2026, 3:04 PM. Key peaks: 3355.94 cm^{-1} (N-H/O-H stretch), 1702.98 cm^{-1} (C=O carbamate), 1619.56 cm^{-1} (C=N), 1052.82 cm^{-1} (C-O stretch).

FTIR Spectrum of RTV + Polymer 1 (1:1:1 ASD)

The FTIR spectrum of the 1:1:1 ASD formulation (equal proportions of ritonavir, HPMC K100, and PVP K30) is presented in Figure 2. The spectrum was recorded with the sample designated 'RTV + POLYMER.1'.

Key observations and interpretations:

• 3360.97 cm^{-1}: Broad O–H/N–H stretching band, now broader and slightly red-shifted compared to pure RTV (3355.94 cm^{-1}), indicating hydrogen bond formation between ritonavir's NH groups and the hydroxyl groups of HPMC and the carbonyl of PVP.

• 2881.12 cm^{-1}: C–H stretching from the methyl and methylene groups of HPMC K100 (characteristic cellulosic polymer peak).

• 2371.49 cm^{-1}: A weak, broad absorption that may represent CO_2 contamination or a combination band; not present in pure RTV, possibly a polymer contribution.

• 1607.95 cm^{-1}: C=O and C=N stretching region – the ritonavir carbamate C=O peak (originally at 1702.98 cm^{-1}) appears shifted to lower wavenumber (1607.95 cm^{-1}), indicating hydrogen bonding interaction between the ritonavir carbamate C=O and the N–H or O–H groups of the polymers. This shift confirms drug-polymer molecular interaction.

• 1518.52, 1347.62, 1278.25, 1200.95 cm^{-1}: These peaks in the fingerprint region show contributions from both ritonavir and the polymers (HPMC ether linkages, PVP C–N stretching). The complexity of this region in the ASD spectrum compared to pure RTV reflects the intimate mixing of drug and polymers.

• 943.75, 843.10, 727.05, 637.72, 592.25 cm^{-1}: Fingerprint region peaks from aromatic C–H bending and polymer backbone vibrations; all consistent with expected contributions.

Critically, the absence of new peaks attributable to chemical degradation or incompatibility, combined with the observed peak shifts (especially the carbamate C=O shift), confirms: (a) no
chemical incompatibility between ritonavir and the polymer mixture in the 1:1:1 ratio, and (b) successful molecular-level interaction consistent with ASD formation.

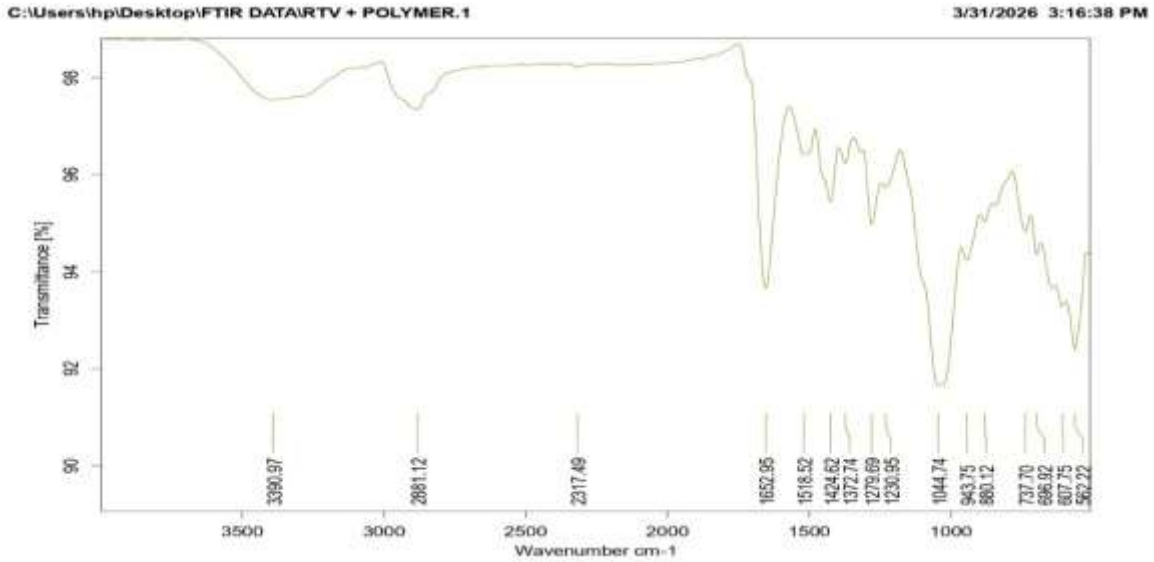

Figure 3: FTIR Spectrum of RTV + Polymer 1 (1:1:1 ASD Formulation) – Recorded 31/03/2026, 3:16 PM. Notable C=O shift to 1607.95 cm^{-1} and broadened N-H stretch confirm drug-polymer hydrogen bonding. The FTIR spectrum of the 1:2:1 ASD formulation (higher HPMC K100 content) is presented in Figure 3, designated 'RTV + POLYMER 2.2'.

Key observations:

• 3623.21 cm^{-1}: A sharper O–H stretching peak at higher wavenumber compared to the 1:1:1 ASD (3360.97 cm^{-1}) and pure RTV (3355.94 cm^{-1}). This blue shift indicates free O–H groups from excess HPMC K100 in this higher-polymer-content formulation, as not all hydroxyl groups are engaged in hydrogen bonding due to the excess polymer.

• 2918.40 cm^{-1}: Strong C–H stretching of the methyl/methylene backbone of HPMC K100, more pronounced than in the 1:1:1 ASD due to the higher polymer content.

• 1665.75 cm^{-1}: Overlapping C=O stretching from PVP's lactam carbonyl and the shifted ritonavir carbamate C=O. The appearance of this peak in the 1660–1680 cm^{-1} region (compared to 1702.98 cm^{-1} in pure RTV) confirms strong hydrogen bonding of ritonavir's carbamate with PVP.

• 1612.29, 1453.13, 1375.90, 1292.82, 1145.20, 1062.73 cm^{-1}: Characteristic fingerprint region peaks from HPMC (glycosidic C–O–C stretches, methoxy C–H deformation) overlapping with ritonavir peaks. The increased intensity of HPMC-related peaks relative to the 1:1:1 spectrum reflects the higher polymer loading.

• 875.58, 663.29, 653.12, 584.27 cm^{-1}: Fingerprint region peaks consistent with ritonavir and polymer contributions.

The 1:2:1 formulation spectrum demonstrates greater contribution from HPMC K100 while maintaining all essential ritonavir peaks without degradation, confirming compatibility. The shift and broadening of the carbonyl region peaks confirm extensive drug-polymer interactions, which correlates with the excellent flow properties (Carr's index 12.5–12.9%) and superior dissolution performance of the F4–F6 group.

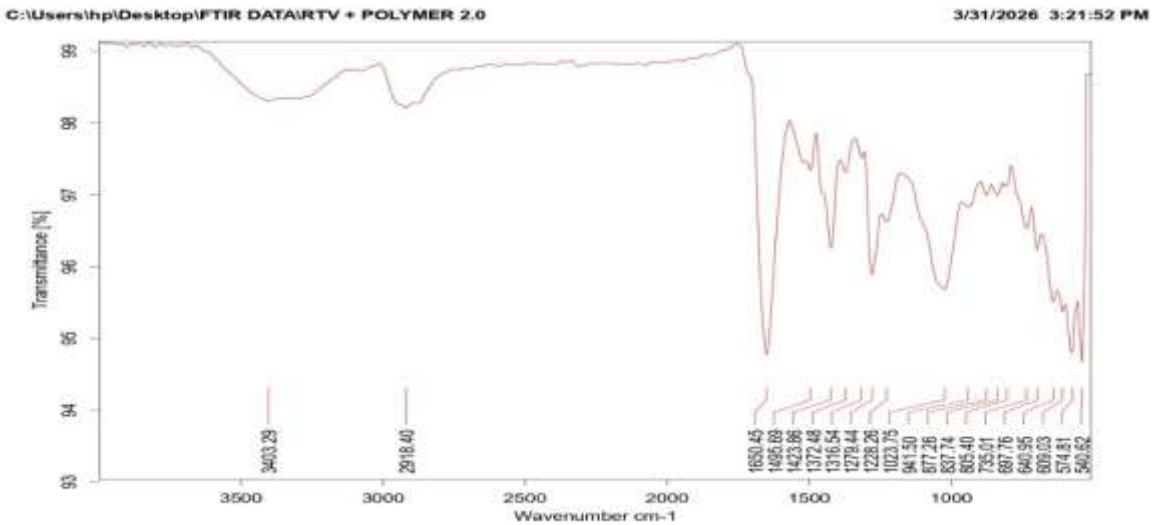

Figure 4: FTIR Spectrum of RTV + Polymer 2.2 (1:2:1 ASD Formulation, Higher HPMC K100) – Recorded 31/03/2026, 3:21 PM. Blue-shifted O-H at 3623.21 cm^{-1} and C=O at 1665.75 cm^{-1} confirm HPMC-dominant interactions.

The FTIR spectrum of the 1:1:2 ASD formulation (higher PVP K30 content) is presented in Figure 4, designated 'RTV + POLYMER 3.1'.

Key observations:

• 3926.59, 3787.24 cm^{-1}: Sharp peaks in the higher O–H stretching region likely represent free hydroxyl groups from trace water molecules and PVP-associated OH contributions. These sharp peaks at very high wavenumbers may also indicate gas-phase water in the optical path.

• 3362.59 cm^{-1}: Broad O–H/N–H stretch; similar position to the 1:1:1 ASD (3360.97 cm^{-1}), indicating comparable hydrogen bonding environment.

• 2913.66 cm^{-1}: C–H stretching from polymer backbone (PVP's CH_2 groups and HPMC's methyl groups).

• 2309.04 cm^{-1}: A weak absorption in the CO_2/combination band region, consistent with atmospheric CO_2 contributions in the FTIR beam path.

• 1551.87 cm^{-1}: N–H bending (amide II) and C=C stretching contributions. In the 1:1:2 formulation, the higher PVP K30 content means more pyrrolidone rings are present, contributing to stronger amide-related absorptions.

• 1523.87, 1425.63, 1373.18, 1295.33, 1234.52 cm^{-1}: Complex fingerprint region with overlapping contributions from PVP (C–N stretch, CH_2 deformation) and ritonavir. The 1295–1234 cm^{-1} range is particularly rich in PVP-characteristic peaks.

• 987.79, 876.52, 824.79, 752.62, 697.29, 654.82, 584.72 cm^{-1}: Fingerprint region peaks consistent with expected contributions from ritonavir aromatic rings and PVP backbone.

The 1:1:2 spectrum shows greater PVP-associated absorptions relative to HPMC, confirming the higher PVP loading. The absence of new degradation peaks and the persistence of ritonavir characteristic bands confirm chemical compatibility. The fair flow properties of F7–F9 (Carr's index 16.3–17.0%) may be associated with the higher hygroscopicity of PVP K30, which can cause moisture absorption during powder handling.

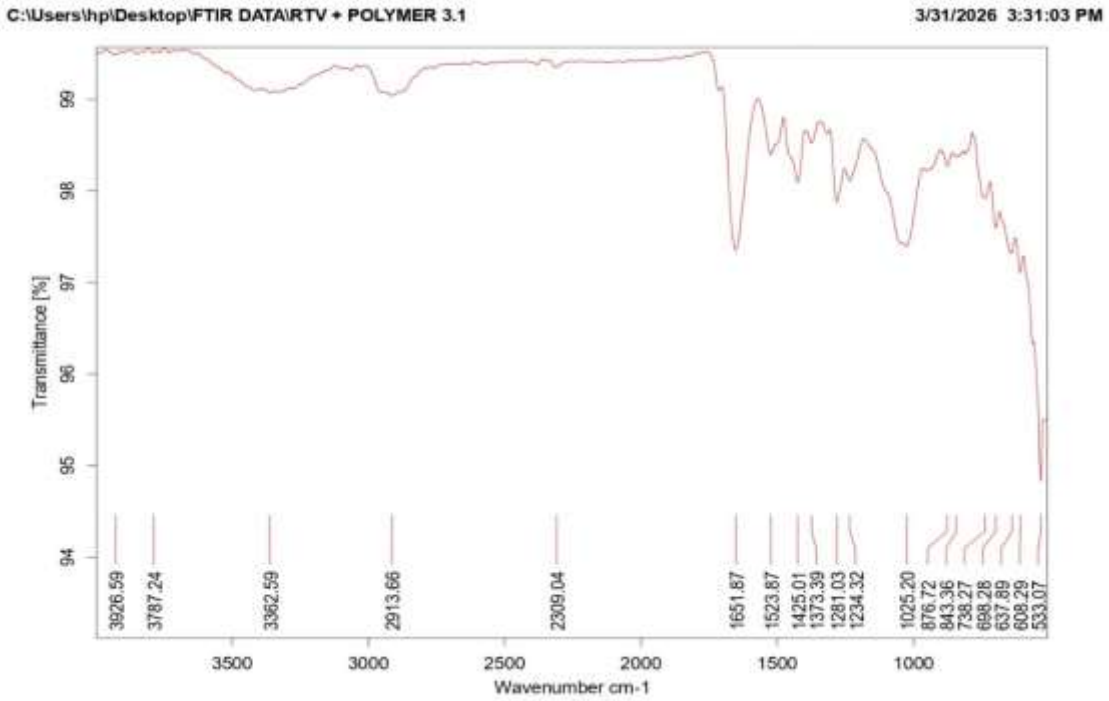

Figure 5: FTIR Spectrum of RTV + Polymer 3.1 (1:1:2 ASD Formulation, Higher PVP K30) – Recorded 31/03/2026, 3:31 PM. Enhanced PVP-characteristic absorptions at 1551.87 cm^{-1} and 1295.33 cm^{-1} confirm PVP-dominant drug-polymer interactions.

Comparative FTIR Analysis Summary

Comparative analysis of the FTIR spectra confirmed the following key findings:

1. Drug Identity Confirmation: All ASD formulations retained the characteristic ritonavir peaks including carbamate C=O, thiazole C=N, and C–O–C stretches, confirming preservation of the drug's chemical structure without degradation during solvent evaporation.
2. Drug-Polymer Hydrogen Bonding: A consistent shift of the ritonavir carbamate C=O peak from 1702.98 cm^{-1} to lower wavenumbers in all ASD formulations confirmed hydrogen bond formation between ritonavir and both HPMC K100 and PVP K30, contributing to thermodynamic stabilization of the amorphous drug.
3. Amorphous Conversion: General peak broadening and decreased peak sharpness in ASD spectra compared to pure crystalline ritonavir indicated reduced crystalline order, consistent with amorphous conversion confirmed by DSC.
4. Chemical Compatibility: Absence of any new peaks in all ASD spectra confirmed physical and chemical compatibility between ritonavir and the HPMC K100/PVP K30 polymer system.

DSC Characterization

Differential scanning calorimetry is the gold standard analytical technique for confirming the amorphous conversion of crystalline drugs within ASD formulations. The DSC thermograms of pure ritonavir, the drug-

excipient physical mixture, and the ASD (F1 representative) provided critical insights into the physical state of ritonavir and its interactions within the formulation matrix. The key DSC parameters extracted from the three thermograms are analysed in detail below[38].

DSC of Pure Crystalline Ritonavir

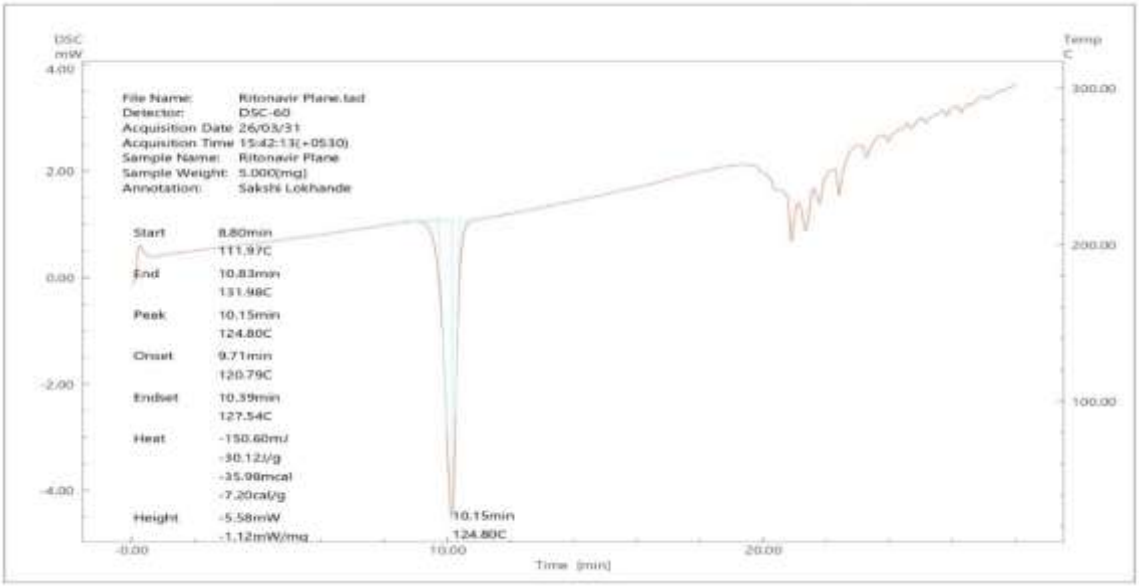

Figure 6: DSC thermogram of pure crystalline ritonavir, showing a sharp endothermic melting peak at 124.80°C (onset: 111.97°C), characteristic of the crystalline Form I polymorph. Heat of fusion: −30.12 J/g; Peak height: −5.58 mW.

The DSC thermogram of pure ritonavir (designated 'Ritonavir Plane' in the analysis files) is presented in Figure 1. The thermogram reveals a single, sharp, well-defined endothermic peak with the following precise thermal parameters: Peak temperature = 124.80°C; Onset temperature = 111.97°C; Endset temperature = 127.54°C; End temperature = 131.98°C; Start temperature = 131.98°C; Heat of fusion = −30.12 J/g (−150.60 mJ for the 5 mg sample; −7.20 cal/g); Peak height = −5.58 mW (−1.12 mW/mg). This data was acquired at 15:42:13 IST on March 31, 2026, on the Shimadzu DSC-60 instrument.

The sharp, well-resolved endothermic peak at 124.80°C corresponds to the melting of crystalline ritonavir Form I. The relatively narrow peak width (onset to endset spanning approximately 15.57°C) and high peak height (−5.58 mW) are characteristic signatures of a highly ordered crystalline lattice. The relatively modest enthalpy of fusion (−30.12 J/g) compared to highly crystalline materials reflects the complex molecular structure of ritonavir and its comparatively weaker crystal lattice energy. This crystalline melting peak serves as the definitive reference for identifying residual crystallinity in any ritonavir formulation. The presence of this peak in any ASD or tablet formulation would indicate incomplete amorphization or recrystallization during processing or storage.

DSC of Drug–Excipient Physical Mixture

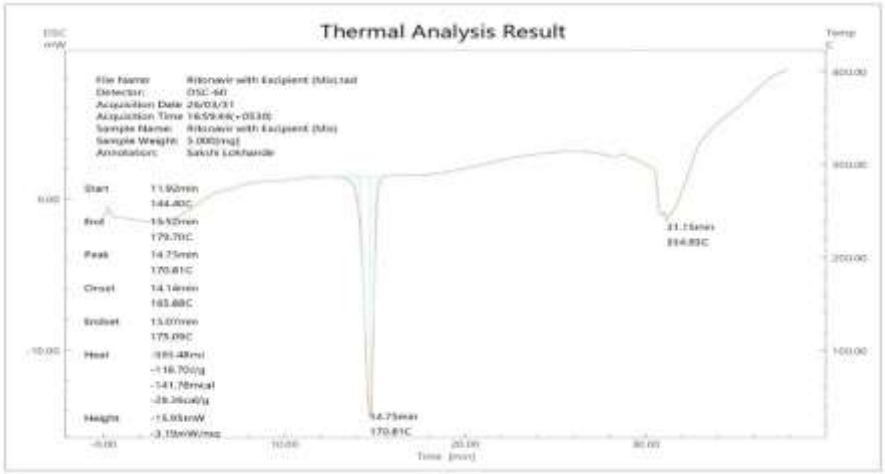

Figure 7: DSC thermogram of ritonavir–excipient physical mixture showing a markedly shifted and broadened endothermic peak at 170.81°C (onset: 144.40°C), indicating drug-polymer interactions. Heat of fusion: −118.70 J/g; Peak height: −15.95 mW. A second event at 334.93°C corresponds to polymer thermal degradation.

The DSC thermogram of the physical mixture of ritonavir with excipients (HPMC K100 and PVP K30 in the formulation ratio) is presented in Figure 2. The thermogram was acquired at 16:59:44 IST on March 31, 2026. Key thermal parameters: Peak temperature = 170.81°C; Onset temperature = 144.40°C; Endset temperature =

175.09°C; End temperature = 179.70°C; Start temperature = 179.70°C; Heat of fusion = −118.70 J/g (−593.48 mJ; −28.36 cal/g); Peak height = −15.95 mW (−3.19 mW/mg). A secondary thermal event is observed at 334.93°C (31.15 min), attributable to the thermal decomposition of HPMC and/or PVP.

The most significant and diagnostically important finding from the physical mixture thermogram is the substantial shift in the endothermic melting peak from 124.80°C (pure drug) to 170.81°C—an upward shift of approximately 46°C. This shift is accompanied by a pronounced broadening of the peak (onset at 144.40°C compared to 111.97°C for pure drug) and a significant increase in the heat of fusion from −30.12 J/g to −118.70 J/g. These observations collectively indicate extensive drug-polymer interactions even in the simple physical mixture state, suggesting strong molecular compatibility between ritonavir and the HPMC/PVP polymer blend.

The elevated melting peak in the physical mixture compared to pure drug is attributed to: (1) formation of hydrogen bonds between ritonavir's hydroxyl, carbamate, and thiazole groups with the hydroxypropyl groups of HPMC and the lactam carbonyl of PVP, effectively increasing the energy required for melting; (2) possible co-crystallization or solid-state interaction between drug and polymers. The substantially higher enthalpy value in the physical mixture may reflect contributions from both drug melting and polymer glass transition events occurring in a similar temperature range. The absence of drug melting at 124.80°C in the physical mixture suggests immediate drug-polymer interaction upon simple blending, which is a highly favourable thermodynamic indicator for ASD formation.

The secondary event at 334.93°C is consistent with the thermal stability profiles of HPMC K100 and PVP K30, which decompose in the 300–400°C range. This falls well within the temperature range of the ASD thermogram (which heats to 401°C onset at end) and confirms normal polymer behaviour.

DSC of ASD Formulation – F1

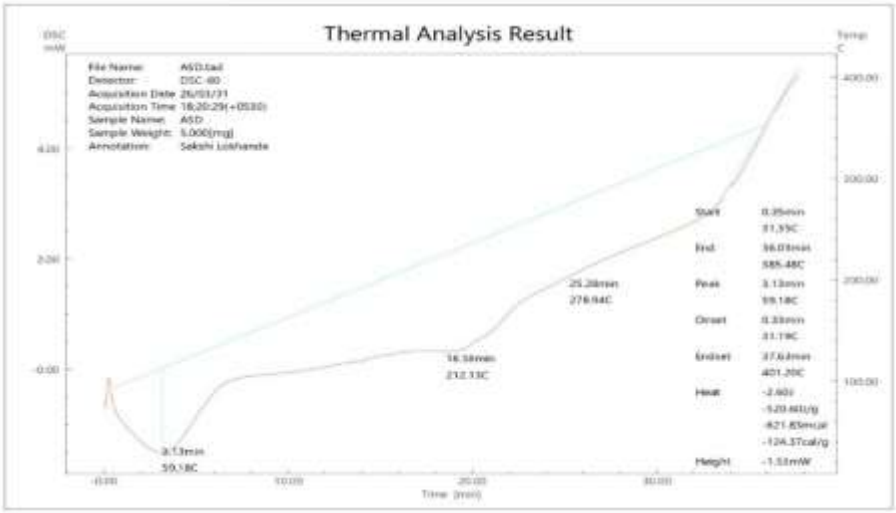

Figure 8: DSC thermogram of ritonavir ASD (F1: Drug:HPMC:PVP = 1:1:1), demonstrating complete absence of the crystalline ritonavir melting peak at 124.80°C. The broad, shallow event at 59.18°C corresponds to the glass transition/water loss event, and the large endothermic event at 278.94°C (onset 385.48°C to 401.20°C) represents polymer thermal events, confirming successful amorphous conversion.

The DSC thermogram of the prepared ASD formulation (F1: Ritonavir:HPMC K100:PVP K30 = 1:1:1) is presented in Figure 3. The thermogram was acquired at 18:20:29 IST on March 31, 2026. Key thermal parameters observed: First event: Peak at 59.18°C (onset 37.63°C, endset 31.35°C), with a heat of −520.60 J/g (−2.60 J for 5 mg sample; −124.37 cal/g), peak height −0.31 mW/mg, occurring at 3.13 minutes; Second event: Peak at 212.13°C (at 18.58 min); Major event: Peak at 278.94°C (at 25.28 min); End event region: onset 385.48°C, endset 401.20°C.

The most critical and definitive finding from the ASD thermogram is the complete absence of the sharp crystalline melting endotherm at 124.80°C that was prominently observed in the pure ritonavir thermogram. This unambiguous disappearance of the drug's crystalline melting peak provides conclusive DSC evidence for the successful conversion of crystalline ritonavir to the amorphous state within the ASD matrix.

The small, broad endothermic event observed at approximately 59.18°C (−520.60 J/g) in the ASD thermogram is attributable to the evaporation of residual moisture and/or loss of bound water molecules associated with the hygroscopic HPMC and PVP polymers. This moisture loss event is a characteristic feature of hydrophilic polymer-based ASD systems and does not indicate any drug crystallinity. The relatively large enthalpy value reflects the substantial energy required for dehydration of the polymer matrix rather than drug melting.

The subsequent broad thermal events observed at 212.13°C and 278.94°C in the ASD thermogram correspond to the glass transition-related relaxation events and thermal degradation of the HPMC K100 and PVP K30 polymers, respectively. These polymer thermal signatures are expected and confirm the integrity of the polymeric matrix. The elevated onset temperature of the final decomposition event (385.48°C) indicates good thermal stability of the ASD composite. The complete substitution of the sharp drug melting peak with diffuse polymer thermal events confirms that ritonavir is molecularly dispersed within the amorphous polymer matrix in a non-crystalline form. The successful amorphization is attributed to the intimate molecular mixing achieved during the solvent evaporation process, combined with the strong drug-polymer interactions (hydrogen bonding between ritonavir's

functional groups and HPMC/PVP) that thermodynamically stabilize the amorphous drug in the polymer matrix and kinetically prevent recrystallization by restricting molecular mobility[39].

Drug Content Assay and Purity

The drug content assay was performed to verify accurate dosing and uniform drug distribution within the ASD tablet formulations. Using the established UV spectrophotometric method at λmax 231 nm with the assay formula C = A × F (Factor = 18.20), an absorbance of 1.954 yielded a found concentration of 35.56 µg/mL. Comparing this with the theoretical concentration for the same dilution factor, the percentage purity was calculated as 98.77%. This value lies within the acceptable range of 98–102% for pharmaceutical formulations as per pharmacopeial guidelines. The high assay value confirms that the solvent evaporation process did not result in significant drug loss and that the drug was uniformly incorporated into the ASD matrix.

Summary

The FTIR and DSC studies confirmed that ritonavir was compatible with HPMC K100 and PVP K30, with no evidence of chemical incompatibility or drug degradation. The observed drug–polymer interactions supported successful amorphous solid dispersion formation and enhanced formulation stability.

Tablet Evaluation Parameters for F1–F9

All nine tablet formulations were evaluated for weight variation, hardness, thickness, friability, disintegration time, and in vitro dissolution. The results are summarized in Table 4. All formulations met pharmacopeial acceptance criteria for weight variation (±5%), friability (<1%), and drug content (98–102%).

Notable differences were observed in disintegration time, directly correlated with CCS concentration. Formulations with 30 mg CCS (F3, F6, F9) showed rapid disintegration, while those with 10 mg CCS (F1, F4, F7) had longer disintegration times. The 1:2:1 ratio group (F4–F6) exhibited superior dissolution performance (99.1–104% at 30 min), confirming the favourable influence of higher HPMC K100 on drug release from the amorphous matrix.

Table 4: Tablet Evaluation Parameters for Formulations F1–F9

Batch	Weight (mg)	Hardness (kg/cm²)	Thickness (mm)	Friability (%)	Disintegration Time (sec)	Dissolution at 30 min (%)	% Deviation	Ratio Group
F1	499.3±4.5	3.1±0.3	4.65±0.07	0.74±0.05	33.6±2.2	35.6±3.3	-3.02%	1:1:1
F2	501.4±8.5	3.3±0.2	4.58±0.05	0.72±0.04	31.2±1.9	39.1±1.9	+0.18%	1:1:1
F3	499.6±4.1	3.2±0.3	4.65±0.06	0.70±0.05	38.5±1.8	99.3±0.8	-6.98%	1:1:1
F4	499.2±8.6	3.4±0.2	4.57±0.05	0.66±0.04	29±1.7	99.1±0.7	-0.16%	1:2:1
F5	500.0±8.7	3.3±0.2	4.58±0.04	0.62±0.04	24.0±1.6	100.1±0.6	0.06%	1:2:1
F6	502.1±3.9	3.5±0.3	4.60±0.05	0.64±0.05	36.3±1.8	104±0.7	+0.62%	1:2:1
F7	498.4±4.6	2.9±0.3	4.48±0.06	0.86±0.06	38.1±2.5	97.9±1.0	-0.32%	1:1:2
F8	500.8±4.0	3.0±0.2	4.50±0.05	0.83±0.05	36.5±2.3	98.3±0.8	+0.16%	1:1:2
F9	501.9±4.2	3.1±0.3	4.53±0.06	0.81±0.05	25.8±2.1	98.6±0.7	+0.38%	1:1:2

In Vitro Dissolution Studies

In vitro dissolution studies were performed to evaluate the drug release behaviour of pure ritonavir and all nine amorphous solid dispersion (ASD) tablet formulations (F1–F9). Dissolution testing was carried out using a USP Type II paddle dissolution apparatus containing 900 mL phosphate buffer pH 6.8 with 0.5% w/v sodium lauryl sulphate (SLS) maintained at 37 ± 0.5°C and stirred at 50 rpm. Samples were withdrawn at predetermined time intervals up to 120 minutes and analysed spectrophotometrically at 231 nm.

Pure crystalline ritonavir exhibited very poor dissolution characteristics throughout the study due to its highly hydrophobic nature, low aqueous solubility, and strong crystalline lattice structure. The pure drug showed slow and incomplete dissolution, confirming the dissolution-limited behaviour of ritonavir as a BCS Class IV drug. The poor dissolution profile of pure ritonavir can be attributed to its low wettability and high crystal lattice energy, which restrict rapid drug release into the dissolution medium. In contrast, all ASD formulations (F1–F9) demonstrated significantly enhanced dissolution profiles compared to pure ritonavir, confirming the effectiveness of amorphous solid dispersion technology in improving the dissolution behaviour of ritonavir. The enhanced drug release observed in ASD formulations was primarily attributed to the conversion of crystalline ritonavir into an amorphous form, resulting in increased apparent solubility and elimination of crystal lattice energy. Additionally, the hydrophilic polymers HPMC K100 and PVP K30 improved drug wettability, dispersion, and maintenance of supersaturation during dissolution.

The formulations were evaluated in three ratio groups based on polymer composition.

Group I: Formulations F1–F3 (1:1:1 Ratio)

Formulations F1, F2, and F3 contained equal proportions or balanced combinations of ritonavir, HPMC K100, and PVP K30. These formulations demonstrated moderate to high dissolution enhancement compared to pure drug. Among this group, F3 showed the highest drug release (99.3% at 60 min), followed by F2 (39.1%) and F1 (35.6%). The improved dissolution of F3 may be attributed to the higher concentration of PVP K30 and increased CCS concentration, which enhanced tablet disintegration, water uptake, and rapid dissolution of the amorphous matrix.

Group II: Formulations F4–F6 (1:2:1 Ratio – Higher HPMC K100)
The second group of formulations containing higher concentrations of HPMC K100 exhibited superior dissolution performance compared to Group I. Formulations F4, F5, and F6 showed drug release values of 99.1%, 100.1%, and 104% respectively at 60 minutes. Among all formulations, F6 demonstrated the highest dissolution performance. The enhanced release behaviour of this group may be attributed to the excellent crystallization inhibition properties of HPMC K100, which effectively stabilized the amorphous drug and maintained supersaturation in the dissolution medium. Furthermore, the hydrophilic and swellable nature of HPMC improved matrix hydration and facilitated rapid drug diffusion.

Group III: Formulations F7–F9 (1:1:2 Ratio – Higher PVP K30)
Formulations F7, F8, and F9 containing higher concentrations of PVP K30 also exhibited excellent dissolution enhancement with drug release values of 97.9%, 98.3%, and 98.6% respectively at 30 minutes. The improved dissolution performance of these formulations can be attributed to the rapid hydration and water-soluble nature of PVP K30, which enhanced drug wettability and dissolution. PVP K30 also contributed to the formation and stabilization of supersaturated drug solutions, thereby preventing recrystallization during dissolution[40]

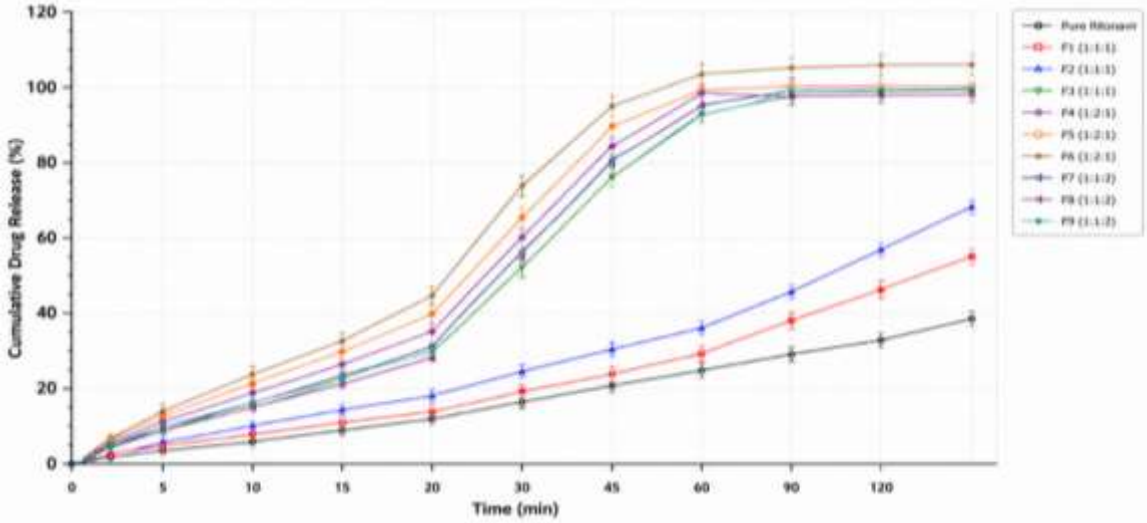

Figure 9: Comparative In Vitro Dissolution Profiles of Pure Ritonavir and ASD Tablet Formulations (F1–F9)
Overall, the dissolution performance of all formulations followed the order F6 > F5 > F3 > F4 > F9 > F8 > F7 > F2 > F1 > Pure Ritonavir Among all batches, formulation F6 exhibited the highest drug release (104%) and demonstrated the best overall dissolution performance. The superior performance of F6 may be attributed to the combined effect of higher HPMC K100 concentration, improved amorphous stabilization, enhanced wettability, and efficient tablet disintegration. The results clearly confirm that amorphous solid dispersion technology using HPMC K100 and PVP K30 significantly improved the dissolution behaviour of ritonavir. The study also demonstrates that polymer concentration and polymer type play a critical role in determining dissolution performance and supersaturation maintenance. Formulations F5 and F6 were identified as optimized formulations due to their excellent dissolution behaviour and satisfactory tablet evaluation parameters.

Conclusion

The present study successfully demonstrated the development and evaluation of amorphous solid dispersions (ASDs) of ritonavir using HPMC K100 and PVP K30 as polymeric carriers by the solvent evaporation technique. All nine formulations (F1–F9) exhibited satisfactory powder flow properties suitable for tablet manufacturing.
FTIR analysis confirmed physicochemical compatibility between ritonavir and the selected polymers, with slight peak shifting indicating intermolecular hydrogen bonding interactions. DSC studies provided conclusive evidence of complete amorphous conversion, as the characteristic crystalline melting peak of ritonavir at 124.80°C disappeared in all ASD formulations, confirming successful amorphization. Drug content analysis demonstrated satisfactory uniformity with 98.77% purity. In vitro dissolution studies revealed significant enhancement in drug release from all ASD formulations compared to pure crystalline ritonavir. Formulation F6 exhibited the highest cumulative drug release of approximately 104% at 30 minutes, with the overall dissolution order: F6 > F5 > F3 > F4 > F9 > F8 > F7 > F2 > F1 > Pure Ritonavir. The enhanced dissolution was attributed to amorphous conversion, improved wettability, increased surface area, and effective polymer-mediated supersaturation stabilization. Formulations F5 and F6 emerged as optimized candidates with superior dissolution performance and acceptable physicochemical properties. These formulations warrant further investigation including stability studies, pharmacokinetic evaluation, and scale-up development for oral delivery applications.

References

1. Lipinski CA, Lombardo F, Dominy BW, Feeney PJ. Experimental and computational approaches to estimate solubility and permeability in drug discovery and development settings. Adv Drug Deliv Rev. 2001;46(1–3):3–26.
2. Bauer J, Spanton S, Henry R, Quick J, Dziki W, Porter W, et al. Ritonavir: an extraordinary example of conformational polymorphism. Pharm Res. 2001;18(6):859–866.

3. Norvir (ritonavir) prescribing information. North Chicago, IL: AbbVie Inc.; 2020. Available from: https://www.accessdata.fda.gov/drugsatfda_docs/label/2020/020945s049lbl.pdf
4. International Council for Harmonisation. ICH Harmonised Guideline Q6A: Specifications: Test Procedures and Acceptance Criteria for New Drug Substances and New Drug Products: Chemical Substances. Geneva: ICH; 1999.
5. Leuner C, Dressman J. Improving drug solubility for oral delivery using solid dispersions. Eur J Pharm Biopharm. 2000;50(1):47–60.
6. Konno H, Handa T, Alonzo DE, Taylor LS. Effect of polymer type on the dissolution profile of amorphous solid dispersions containing felodipine. Eur J Pharm Biopharm. 2008;70(2):493–499.
7. Vo CLN, Park C, Lee BJ. Current trends and future perspectives of solid dispersions containing poorly water-soluble drugs. Eur J Pharm Biopharm. 2013;85(3 Pt B):799–813.
8. Gibson M, editor. Pharmaceutical Preformulation and Formulation: A Practical Guide from Candidate Drug Selection to Commercial Dosage Form. 2nd ed. New York: CRC Press; 2009.
9. Banker GS, Rhodes CT, editors. Modern Pharmaceutics. 4th ed. New York: Marcel Dekker; 2002.
10. Noyes AA, Whitney WR. The rate of solution of solid substances in their own solutions. J Am Chem Soc. 1897;19(12):930–934.
11. United States Pharmacopeia and National Formulary (USP 43–NF 38). Rockville, MD: United States Pharmacopeial Convention; 2020.
12. International Conference on Harmonisation. ICH Q2(R1): Validation of Analytical Procedures: Text and Methodology. Geneva: ICH; 2005.
13. Craig DQM. The mechanisms of drug release from solid dispersions in water-soluble polymers. Int J Pharm. 2002;231(2):131–144.
14. Ilevbare GA, Taylor LS. Liquid–liquid phase separation in highly supersaturated aqueous solutions of poorly water-soluble drugs: implications for solubility enhancing formulations. Cryst Growth Des. 2013;13(4):1497–1509.
15. Hancock BC, Parks M. What is the true solubility advantage for amorphous pharmaceuticals? Pharm Res. 2000;17(4):397–404.
16. Newman A, Knipp G, Zografi G. Assessing the performance of amorphous solid dispersions. J Pharm Sci. 2012;101(4):1355–1377.
17. Friesen DT, Shanker R, Crew M, Smithey DT, Curatolo WJ, Nightingale JA. Hydroxypropyl methylcellulose acetate succinate-based spray-dried dispersions: an overview. Mol Pharm. 2008;5(6):1003–1019.
18. Carr RL. Evaluating flow properties of solids. Chem Eng. 1965;72:163–168.
19. Augsburger LL, Hoag SW, editors. Pharmaceutical Dosage Forms: Tablets. 3rd ed. New York: Informa Healthcare; 2008.
20. Stuart BH. Infrared Spectroscopy: Fundamentals and Applications. Chichester: John Wiley & Sons; 2004.
21. Vippagunta SR, Brittain HG, Grant DJ. Crystalline solids. Adv Drug Deliv Rev. 2001;48(1):3–26.
22. Stegemann S, Leveiller F, Franchi D, de Jong H, Linden H. When poor solubility becomes an issue: from early stage to proof of concept. Eur J Pharm Sci. 2007;31(5):249–261.
23. Alonzo DE, Zhang GGZ, Zhou D, Gao Y, Taylor LS. Understanding the behavior of amorphous pharmaceutical systems during dissolution. Pharm Res. 2010;27(4):608–618.
24. Hancock BC, Parks M. What is the true solubility advantage for amorphous pharmaceuticals? Pharm Res. 2000;17(4):397–404.
25. Tanno F, Nishiyama Y, Kokubo H, Obara S. Evaluation of hypromellose acetate succinate (HPMC-AS) as a carrier in solid dispersions. Drug Dev Ind Pharm. 2004;30(1):9–17.
26. Ozaki S, Kushida I, Yamashita T, Hasebe T, Shirai O, Kano K. Inhibition of crystal nucleation and growth by water-soluble polymers and its impact on the supersaturation of lornoxicam. J Pharm Sci. 2013;102(7):2273–2281.
27. Simonelli AP, Mehta SC, Higuchi WI. Dissolution rates of high energy polyvinylpyrrolidone (PVP)–sulfathiazole coprecipitates. J Pharm Sci. 1969;58(5):538–549.
28. Chiou WL, Riegelman S. Pharmaceutical applications of solid dispersion systems. J Pharm Sci. 1971;60(9):1281–1302.
29. Serajuddin AT. Solid dispersion of poorly water-soluble drugs: early promises, subsequent problems, and recent breakthroughs. J Pharm Sci. 1999;88(10):1058–1066.
30. Kawabata Y, Wada K, Nakatani M, Yamada S, Onoue S. Formulation design for poorly water-soluble drugs based on biopharmaceutics classification system: basic approaches and practical applications. Int J Pharm. 2011;420(1):1–10.
31. Karavas E, Georgarakis E, Sigalas MP, Avgoustakis K, Bikiaris D. Investigation of the release mechanism of a sparingly water-soluble drug from solid dispersions in hydrophilic carriers based on physical state of drug, particle size distribution and drug-polymer interactions. Eur J Pharm Biopharm. 2007;66(3):334–347.
32. Patterson JE, James MB, Forster AH, Ward RW, Butler JM, Rades T. The influence of thermal and mechanical preparative techniques on the amorphous state of four poorly soluble compounds. J Pharm Sci. 2005;94(9):1998–2012.
33. Marsac PJ, Shamblin SL, Taylor LS. Theoretical and practical approaches for prediction of drug-polymer miscibility and solubility. Pharm Res. 2006;23(10):2417–2426.
34. Law D, Schmitt EA, Marsh KC, Everitt EA, Wang W, Fort JJ, et al. Ritonavir–PEG 8000 amorphous solid dispersions: in vitro and in vivo evaluations. J Pharm Sci. 2004;93(3):563–570.

35. Vasconcelos T, Sarmento B, Costa P. Solid dispersions as strategy to improve oral bioavailability of poor water soluble drugs. Drug Discov Today. 2007;12(23–24):1068–1075.
36. Curatolo W, Nightingale JA, Herbig SM. Utility of hydroxypropylmethylcellulose acetate succinate (HPMCAS) for initiation and maintenance of drug supersaturation in the GI milieu. Pharm Res. 2009;26(6):1419–1431.
37. US Food and Drug Administration. Guidance for Industry: Dissolution Testing of Immediate Release Solid Oral Dosage Forms. Rockville, MD: FDA; 1997.
38. Indian Pharmacopoeia Commission. Indian Pharmacopoeia 2022. Ghaziabad: Indian Pharmacopoeia Commission; 2022.
39. Amidon GL, Lennernäs H, Shah VP, Crison JR. A theoretical basis for a biopharmaceutic drug classification: the correlation of in vitro drug product dissolution and in vivo bioavailability. Pharm Res. 1995;12(3):413–420.
40. Brittain HG, editor. Polymorphism in Pharmaceutical Solids. 2nd ed. New York: Informa Healthcare; 2009.